

**PFC/JA-87-22**

**Ion Bernstein Wave Heating and Improved  
Confinement on the Alcator C Tokamak**

**J. D. Moody<sup>†</sup>, M. Porkolab<sup>†</sup>, C. L. Fiore,  
F. S. McDermott, Y. Takase, J. Terry, S. M. Wolfe**

**Plasma Fusion Center  
Massachusetts Institute of Technology  
Cambridge, MA 02139**

**June 1987**

**<sup>†</sup> Also Department of Physics, MIT**

**Submitted to: Physical Review Letters**

**This work was supported by the U. S. Department of Energy Contract No. DE-AC02-78ET51013. Reproduction, translation, publication, use and disposal, in whole or in part by or for the United States government is permitted.**

**By acceptance of this article, the publisher and/or recipient acknowledges the U. S. Government's right to retain a non-exclusive, royalty-free license in and to any copyright covering this paper.**

# Ion Bernstein Wave Heating and Improved Confinement on the Alcator C Tokamak

J. D. Moody<sup>†</sup>, M. Porkolab<sup>†</sup>, C. L. Fiore, F. S. McDermott

Y. Takase, J. Terry, and S. M. Wolfe

*Plasma Fusion Center, Massachusetts Institute of Technology*

*Cambridge, MA 02139*

Plasma heating by directly launched ion Bernstein waves (IBW) is investigated in the Alcator C tokamak at densities  $\bar{n}_e \gtrsim 1 \times 10^{20} \text{ m}^{-3}$ . For injected rf powers  $P_{\text{rf}} \lesssim 180 \text{ kW}$ , bulk ion temperature increases of  $\Delta T_i \lesssim 380 \text{ eV}$ , as well as improvements in global particle and central impurity confinement times by a factor of 2–3 are observed. In certain regimes, the energy confinement time improves relative to the initial Ohmic value. At higher densities ( $\bar{n}_e \gtrsim 2 \times 10^{20} \text{ m}^{-3}$ ), the heating ceases to be efficient.

PACS numbers: 52.50.Gj, 52.55.Fa, 52.40.Fd

Radio frequency power absorption in the ion cyclotron range of frequencies is currently being studied as a supplementary method of heating plasmas to fusion temperatures. Recently, Ono and coworkers<sup>1,2</sup> demonstrated efficient heating of ions at low plasma density ( $\bar{n}_e \lesssim 4 \times 10^{19} \text{ m}^{-3}$ ) by absorption of directly launched ion Bernstein waves (IBW). We report in this letter that both significant ion heating and improvements in global particle and central impurity confinement times are observed during IBW injection into higher density ( $\bar{n}_e \gtrsim 5 \times 10^{19} \text{ m}^{-3}$ ) Alcator C tokamak discharges. However, at very high densities ( $\bar{n}_e > 2 \times 10^{20} \text{ m}^{-3}$ ), the heating becomes inefficient. It is believed that the lack of wave penetration and limitation of power injection to  $P_{\text{rf}} \lesssim 100 \text{ kW}$  in such high density plasmas is the cause of the loss of heating.

Ion Bernstein waves are launched from a stainless steel, center fed, T-shaped, movable loop antenna with the center conductor aligned along the direction of the toroidal magnetic field and surrounded by a double layer, molybdenum coated

---

<sup>†</sup> Also Department of Physics, MIT

Faraday shield. The experiments were conducted under the following conditions: rf frequency  $f = 183.6$  MHz; plasma minor radius (set by molybdenum limiters)  $a = 0.115$  m,  $0.12$  m, or  $0.125$  m ; major radius  $R_0 = 0.64$  m; hydrogen majority plasma with a deuterium minority  $0.1\% \lesssim n_D/(n_{H+D}) \lesssim 20\%$ ; toroidal magnetic field strength  $4.8 \text{ T} \leq B_0 \leq 11 \text{ T}$ ; line-averaged electron density  $0.5 \leq \bar{n}_e \leq 4 \times 10^{20} \text{ m}^{-3}$ ;  $P_{\text{rf}} \leq 180 \text{ kW}$ ; plasma current  $160 \text{ kA} \leq I_p \leq 260 \text{ kA}$ ; and  $Z_{\text{eff}} \simeq 2 - 3$ .

Absorption of ion Bernstein waves due to ion cyclotron damping is predicted by linear theory to occur where  $\omega = n\omega_{cj}$  ( $n$  integer,  $j$  particle species). Nonlinear Landau damping may occur where  $\omega = \frac{1}{2}(2m + 1)\omega_{cj}$  ( $m$  integer) and is predicted to dominate linear damping even in the presence of a minority species.<sup>3</sup> Calculated values of the nonlinear threshold power for a single ion species plasma at several central magnetic field values are in the range  $P_{\text{th}} \sim 10\text{-}40 \text{ kW}$ , and are given in Ref. 4.

Central ion temperature increases ( $\Delta T_i/T_i \gtrsim 0.1$ ) of the Hydrogen majority component were observed on Alcator C for magnetic fields in the range  $5 \text{ T} \leq B_0 \leq 11 \text{ T}$  during rf power injection. Although the greatest ion temperature increase was observed at  $B_0 = 9.3 \text{ T}$ , heating occurred over a broad range of magnetic fields ( $2.4 \leq \omega/\omega_{cH(0)} \leq 1.1$ ) and was not strongly dependent on having a particular ion cyclotron resonance located near the plasma center. The majority of heating studies were conducted in sawtooth discharges at  $B_0 \simeq 7.6 \text{ T}$ ,  $5.1 \text{ T}$ , and  $9.3 \text{ T}$ .

At a central magnetic field strength of  $B_0 = 7.6 \text{ T}$  we observe centrally peaked radial ion temperature profiles for both the hydrogen majority and deuterium minority component at  $\bar{n}_e \sim (0.8 - 1) \times 10^{20} \text{ m}^{-3}$ ,  $n_D/n_{H+D} \sim 10\%$ . The hydrogen temperature increased by an amount  $\Delta T_H \approx 200 \text{ eV}$  and the line-averaged electron density increased by  $\sim 20\%$  with  $100 \text{ kW}$  of IBW injected into the plasma. A mass-resolving charge exchange neutral analyzer, which was scanned radially on a shot-to-shot basis to measure ion temperature profiles, showed a thermal energy spectrum for hydrogen both before and during rf injection. The deuterium

component also exhibited a thermal energy spectrum during rf injection with an effective temperature (obtained from deuterium particle flux at energies  $E \geq 4$  keV) of approximately 1.3 keV on axis, somewhat hotter than the background heated hydrogen temperature of 0.9 keV. At  $B_0 = 7.6$  T, we expect rf power absorption at the  $\omega/\omega_{cH} = 3/2$  resonance layer located at  $x/a = -0.3$ , about 3.4 cm to the high field side of the plasma axis ( $x = R - R_0$ ). Ray tracing and power absorption calculations in this regime indicate that both nonlinear absorption on hydrogen and linear absorption on deuterium may be important here.

In Fig. 1 we show that the ion temperature increase at  $B = 7.6$  T follows an ion heating rate of 2.3 eV/kW at  $\bar{n}_e = 1 \times 10^{20} \text{ m}^{-3}$ . It is possible to estimate that the collisional power transfer from the heated deuterium component to the background hydrogen is  $\lesssim 30$  kW; however, this estimate is strongly dependent on the fraction of deuterium in the discharge and also on the radial temperature profile and is uncertain to within a factor of 2. The hydrogen temperature increase appears to show a power threshold of 35 kW at the onset of ion heating which is consistent with the threshold estimated for 60% single pass absorption of the injected rf power.<sup>4</sup> Surprisingly, there is also a power threshold of about 30 kW for the high energy deuterium component.<sup>5</sup> Presently, this threshold is not well understood.

At a central magnetic field strength of  $B_0 = 5.1$  T the  $\omega/\omega_{cH} = 5/2$  ( $\omega/\omega_{cD} = 5$ ) resonance layer is located at  $x/a = 0.3$ . In this regime we find a heating rate of 2.2 eV/kW, (see Fig. 1) similar to the 7.6 T case. The calculated power threshold<sup>4</sup> is  $\sim 30$  kW, in good agreement with experimental observations (there was no observable heating below this power). At  $B = 5.1$  T, the temperature increase of the hydrogen majority and deuterium minority ions is thermal ( $T_H = T_D$ ) and is independent of deuterium concentration, suggesting that nonlinear absorption on hydrogen is dominant in this regime.

The most efficient heating is observed when the magnetic field is increased to high values ( $B_0 \gtrsim 9$  T). Here, the analysis is more complicated, and, to our

knowledge, this regime has not been explored in previous experiments. For example, at a field of  $B_0 = 9.3\text{ T}$  the  $\omega/\omega_{cD} = 5/2$  minority subharmonic resonance layer is located on the high magnetic field side of the plasma axis at  $x/a = -0.18$  ( $a = 0.12\text{ m}$ ). However, the  $\omega/\omega_{cH} = 3/2$  and  $\omega/\omega_{cD} = 3$  layer is at  $x/a = 0.85$ , approximately 2 cm in front of the antenna. Ray tracing and power absorption calculations show that ion Bernstein wave absorption should be complete by either mechanism at the plasma edge ( $x/a = 0.85$ ). Using  $\text{CO}_2$  laser scattering techniques, a strong attenuation in wave power in the range  $40 < k_\perp \leq 140\text{ cm}^{-1}$  is observed across the  $\omega/\omega_{cD} = 3/2$  layer.<sup>6</sup> However, as is shown in Fig. 1, an ion heating rate of 4.1 eV/kW at  $\bar{n}_e = 1 \times 10^{20}\text{ m}^{-3}$  is observed with a very low power threshold ( $0 \lesssim P_{\text{th}} \lesssim 10\text{ kW}$  within experimental error). To further complicate matters, the deuterium component has a two temperature energy spectrum with a superthermal component at  $T_D = 2\text{ keV}$ . The radial temperature profile of the deuterium is centrally peaked on the plasma axis. The temporal temperature evolution indicates that the deuterium achieves its maximum temperature before the hydrogen, and both exhibit a slow decay time of about 5 ms after rf power shut-off, indicating central nonlinear rf heating of the deuterium species at the  $\omega/\omega_{cD} = 5/2$  layer. To explain the energetic deuterium component, at least a fraction of the rf power must penetrate to the plasma interior. One possible mechanism for this is the variation in the toroidal field caused by the toroidal field ripple. The presence of the access port in Alcator C perturbs the toroidal field current causing a toroidal field ripple of about 2–4% near the IBW antenna. Consequently, the  $\omega/\omega_{cD} = 3$  layer may be located 2 cm in front of the antenna at the port location but may be positioned behind the Faraday shield at either end of the antenna, away from the port (the port is 4 cm wide and the antenna is 25 cm long). Thus, power from either end of the antenna may freely propagate to the plasma center and heat the deuterium. Another possible mechanism is that the linear resonance at  $\omega/\omega_{cD} = 3$  may become smeared out due to strong particle orbit perturbations resulting from large electric fields near this resonance. Only partial absorption of power would then occur at

$\omega/\omega_{cD} = 3$  and a significant fraction of rf power could still propagate into the plasma center. Nonlinear absorption by the deuterium minority species is possible above a threshold power of  $\sim 30$  kW for  $n_D/n_H = 0.02$  (the threshold power is inversely proportional to the deuterium concentration).

Improvements in  $\tau_p$ , the global particle confinement time of up to 3 times its value in the Ohmically heated plasma are often observed for  $\bar{n}_e < 2.5 \times 10^{20} \text{ m}^{-3}$ . The global particle confinement time,  $\tau_p$ , is calculated by dividing the total number of electrons  $N_e$  by  $S - dN_e/dt$ , where  $S$  is the source rate of electrons at the plasma edge as inferred from  $H_\alpha$  measurements. Figure 2(a) shows a strong dependence of  $\tau_{p(\text{rf})}/\tau_{p(\text{Ohmic})}$  on target plasma density with a maximum of  $\tau_{p(\text{rf})}/\tau_{p(\text{Ohmic})} = 3.4$  at  $\bar{n}_e = 0.6 \times 10^{20} \text{ m}^{-3}$  and decreasing to unity for  $\bar{n}_e > 2.5 \times 10^{20} \text{ m}^{-3}$ . Improvements in  $\tau_p$  are observed over a wide range of toroidal fields  $4.8 \text{ T} \leq B \leq 10.4 \text{ T}$ ; however, the most significant improvement in  $\tau_p$  occurs in the 9.3 T regime where the  $\omega = 3\omega_{cD}$  resonance layer is located at the plasma edge. Here, the line averaged electron density typically increases by up to 100% and the source rate  $S$  (as determined from  $H_\alpha$  measurements) decreases by about 30% during IBW injection. Several non-rf discharges in which the density was increased by gas puffing alone were compared with rf discharges. These all showed fractional increases in the  $H_\alpha$  intensity which were larger than the fractional increases in the density, indicating decreasing particle confinement in the absence of rf power injection.

Central impurity confinement times were also observed to increase by factors of 2–3 during IBW injection. This was measured by injecting trace amounts of Silicon using the laser blow-off technique.<sup>7</sup> The brightness of He-like Si (an ionization state which exists in the center of these discharges) is observed to decay at a significantly slower rate in rf heated plasmas. Typical values of  $\tau_{\text{Si}}$  corresponding to before (Ohmic), during, and after IBW injection in the 9.3 T regime are 7, 16–20, and 6 ms. The  $Z_{\text{eff}}$  is typically constant or decreasing during rf injection in these discharges.

A systematic study of ion heating versus target density was carried out. A strong decrease in the ion heating rate was observed for target plasma densities

$\bar{n}_e \gtrsim 1.1 \times 10^{20} \text{ m}^{-3}$ , and as shown in Fig. 2(b), significant increases in the ion temperature were not seen for target densities  $\bar{n}_e > 2.5 \times 10^{20} \text{ m}^{-3}$  and at rf powers  $P_{\text{rf}} \lesssim 100 \text{ kW}$  ( $4.8 \text{ T} < B_0 < 11 \text{ T}$ ). The increases in  $T_i$  for  $\bar{n}_e > 2.5 \times 10^{20} \text{ m}^{-3}$  are within the experimental error of  $\Delta T_i \simeq 0$ . In particular, at high densities it was difficult to inject more than  $\sim 100 \text{ kW}$  from the antenna ( $P/A \sim 1 \text{ kW/cm}^2$ ). The nonlinear power threshold, which increases linearly with increasing plasma density, can in principle explain the decrease in heating efficiency. However, the decrease is more sudden than expected and linear damping of IBW on the deuterium minority should still occur even at high density. Furthermore, the scattered  $\text{CO}_2$  signal<sup>6</sup> from IBW also exhibited a sharp decrease above  $\bar{n}_e \simeq 1 \times 10^{20} \text{ m}^{-3}$ . When the  $\text{CO}_2$  scattering diagnostic was reconfigured to measure low frequency edge density fluctuations as a function of plasma density, the measurements showed a minimum in edge scattered signal which corresponded to a maximum in central IBW scattered signal. These results suggest that the decrease in ion heating may partially be attributed to inaccessibility of the IBW to the plasma center due to scattering from edge density fluctuations ( $\delta n/n \gtrsim 0.3$  at  $r/a \simeq 0.9$ ) as the target density is increased.

Figure 3 shows the change in total stored energy,  $\Delta W_t$  versus the change in total input power,  $\Delta P_t$  during IBW heating at  $B = 9.3 \text{ T}$ . When calculating the total stored energy and input power, the temperature and density profiles are assumed constant in both the rf and Ohmic heated portions of the discharge. All discharges represented in the figure have initial Ohmic energy confinement times,  $\tau_{\text{B(Oh)}} = 5.6 \pm 0.8 \text{ ms}$ , and rf confinement times,  $\tau_{\text{B(rf)}} = 6.5 \pm 1.2 \text{ ms}$ . The incremental energy confinement time, which is defined as  $\Delta W_t / \Delta P_t$ , has an average value of  $15.5 \text{ ms}$ , for discharges with very low deuterium concentration and ranges between  $3.9 \text{ ms}$  and  $17.5 \text{ ms}$  for discharges with  $n_D/n_H + n_D \leq 20\%$ . The improvement in  $\tau_{\text{B}}$  (with respect to the initial Ohmic confinement time) during rf heating results from the large increase in total energy caused by both strong heating of ions and nearly doubling the plasma density. The Ohmic confinement time at densities similar to

those reached during rf injection is  $\tau_{B(\text{Oh})} = 8.8 \pm 1.2$  ms. At  $B = 7.6$  T there are also improvements in  $\tau_{B}$  during rf injection (with respect to the initial Ohmic  $\tau_{B}$ ).

The results obtained at 9.3 T show some remarkable similarities to H-mode type discharges.<sup>8</sup> For example, the energy and particle confinement times improve, the stored energy and line averaged density increase, and the  $H_{\alpha}$  signal decreases. There are also some marked differences: No clear L-mode phase or delay time to H-mode transition, no measured power or lower density threshold, no separatrix, and no indication of edge localized modes (ELMS).

In order to gain a better understanding of the underlying physics, we have attempted to determine the near edge ion temperature ( $r/a \approx 0.9$ ) as a function of plasma density, during rf injection. These results were obtained from  $\text{CO}_2$  scattering at  $B = 9.3$  T by fitting the ion Bernstein wave dispersion relation to the measured value of  $k_{\perp}$ .<sup>9,10</sup> The maximum edge ion temperature occurred at the same density as the minimum in edge density fluctuations and the maximum in particle confinement improvement ( $\bar{n}_e \simeq 1 \times 10^{20} \text{ m}^{-3}$ ). This density also coincides with that where the central ion heating is most efficient (see Fig. 2(b)). The edge ion temperature at these densities showed an increase with time during the rf pulse (by up to 50%). At higher densities ( $\bar{n}_e > 2 \times 10^{20} \text{ m}^{-3}$ ) the edge ion temperature was significantly lower. There is a large uncertainty in the actual value of the edge ion temperature which is due to complications caused by the presence of the minority deuterium species and the proximity of the  $\omega/\omega_{\text{cD}} = 3$  layer to the scattering volume. At the lower densities, an edge ion temperature near the estimated upper bound of  $T_i$  ( $\simeq 300$  eV) may yield  $\nu_i^* \lesssim 1$  (with large uncertainty), where  $\nu_i^*$  is the ion collisionality parameter.<sup>11</sup> The nearly collisionless regime for ions ( $\nu_i^* \lesssim 1$ ) may be in agreement with the recent theoretical prediction of Hinton for H-mode type phenomena.<sup>12</sup> Measurements of the O-v temperature at  $r/a \simeq 1.0$  and  $B = 7.6$  T were made using a vacuum ultraviolet spectrometer.<sup>13</sup> The measurements showed an increase in the O-v temperature from 75 eV to 95 eV for a density increase from  $\bar{n}_e = 0.9 \times 10^{20} \text{ m}^{-3}$  to  $1.5 \times 10^{20} \text{ m}^{-3}$ . At higher Ohmic densities ( $\bar{n}_e > 2.2 \times 10^{20} \text{ m}^{-3}$ ) no change was



observed in the O-V temperature from its Ohmic value of 65 eV. Spectroscopic measurements at  $B_0 = 9.3$  T are not available.

Edge floating potential measurements in the scrape-off layer  $1.05 \leq r/a \leq 1.2$  were also made using a double Langmuir probe and a gridded energy analyzer.<sup>14</sup> Both probes were toroidally separated from the antenna by a limiter and were at different poloidal locations. During rf power injection, the floating potential usually decreased from an initial Ohmic value of  $\sim -2$  V to  $\sim -10$  V but almost never decreased to less than  $\sim -17$  V. In the same region  $T_e \sim 10$ -30 eV. The variation of the potential inside the limiter edge is not known.

In conclusion, at  $P_{rf} < P_{Oh}$  we have demonstrated very efficient ion heating ( $\bar{n}_e \Delta T_i(0)/P_{rf} \lesssim 45$  eV/kW $10^{19}$  m<sup>-3</sup>) via ion Bernstein wave injection. An improvement in the global particle, and central impurity confinement times (by factors of up to three) accompany this type of rf heating. The consequence of these results is the attainment of good global energy confinement.

The authors would like to thank the Alcator scientific and technical staff for their help in these investigations, and special thanks are due to Dave Griffin for his expert engineering support. This work was supported by the U.S. Department of Energy under contract No. DE-AC02-78ET51013.

## REFERENCES

1. M. Ono, T. Watari, R. Ando, *et al.*, *Phys. Rev. Lett.* **54**, 2339 (1985).
2. M. Ono, *et al.* *Plasma phys. and Contr. Nucl. Fusion Res.* (IAEA 11th Int. Conf., Kyoto, 1986) IAEA-CN-47 / F-I-3.
3. M. Porkolab, *Phys. Rev. Lett.*, **54**, 434 (1985).
4. M. Porkolab, *et al.*, *Plasma Phys. and Contr. Nucl. Fusion Res.* (IAEA 11th Int. Conf., Kyoto, 1986) IAEA-CN-47 / F-II-2.
5. C. L. Fiore, *et al.* 7th Topical Conf. on RF Plasma Heating, Kissimmee, FL, (1987).
6. Y. Takase, *et al.*, *Bull. Am. Phys. Soc.*, **31**, 1587 (1986). MIT Plasma Fusion Center Report PFC/JA-86-60 (1986).
7. E. S. Marmor, J. L. Cecchi, and S. A. Cohen, *Rev. Sci. Instrum.*, **46**, 1149 (1975).
8. F. Wagner, G. Becker, K. Behringer, *et al.*, *Phys. Rev. Lett.*, **49**, 1408 (1982).
9. G. A. Wurden, M. Ono, and K. L. Wong, *Phys. Rev. A*, **26**, 2297 (1982).
10. H. Park, P. S. Lee, W. A. Peebles, N. C. Luhmann, Jr., *Nucl. Fusion*, **25**, 1399 (1985).
11. F. L. Hinton and R. D. Hazeltine, *Rev. Mod. Phys.*, **48**, 239 (1976).
12. F. L. Hinton, *Nucl. Fusion*, **25**, 1457 (1985).
13. R. D. Benjamin, *et al.*, *Bull. Am. Phys. Soc.*, **31**, 1587 (1986).
14. A. Wan, MIT Plasma Fusion Center Report PFC/RR-86-13 (1986).

## Figure Captions

Fig. 1. Ion heating  $\Delta T_i$  as a function of rf power  $P_{\text{rf}}$  for three magnetic field strengths. Each field indicates that a particular resonance is near the plasma center:  $\omega/\omega_{\text{cH}} = 5/2$  at  $B = 5.1$  T,  $\omega/\omega_{\text{cH}} = 3/2$  at  $B = 7.6$  T, and  $\omega/\omega_{\text{cD}} = 5/2$  at  $B = 9.3$  T.

FIG. 2a. Comparison of particle confinement time for ohmic and ohmic plus IBW heated plasma as a function of the line-averaged density of the pre-rf, ohmically heated plasma.

FIG. 2b. Hydrogen ion heating rate,  $\Delta T_i(0)/P_{\text{rf}}$  (eV/kW), as a function of the line-averaged density during rf injection.

FIG. 3. Increase in total plasma thermal energy,  $\Delta W_t$ , as a function of  $\Delta P_t$ , the change in total (rf plus ohmic) input power. The dashed lines show the incremental energy confinement time  $\tau_{\text{inc}} \equiv \Delta W_t/\Delta P_t$ .

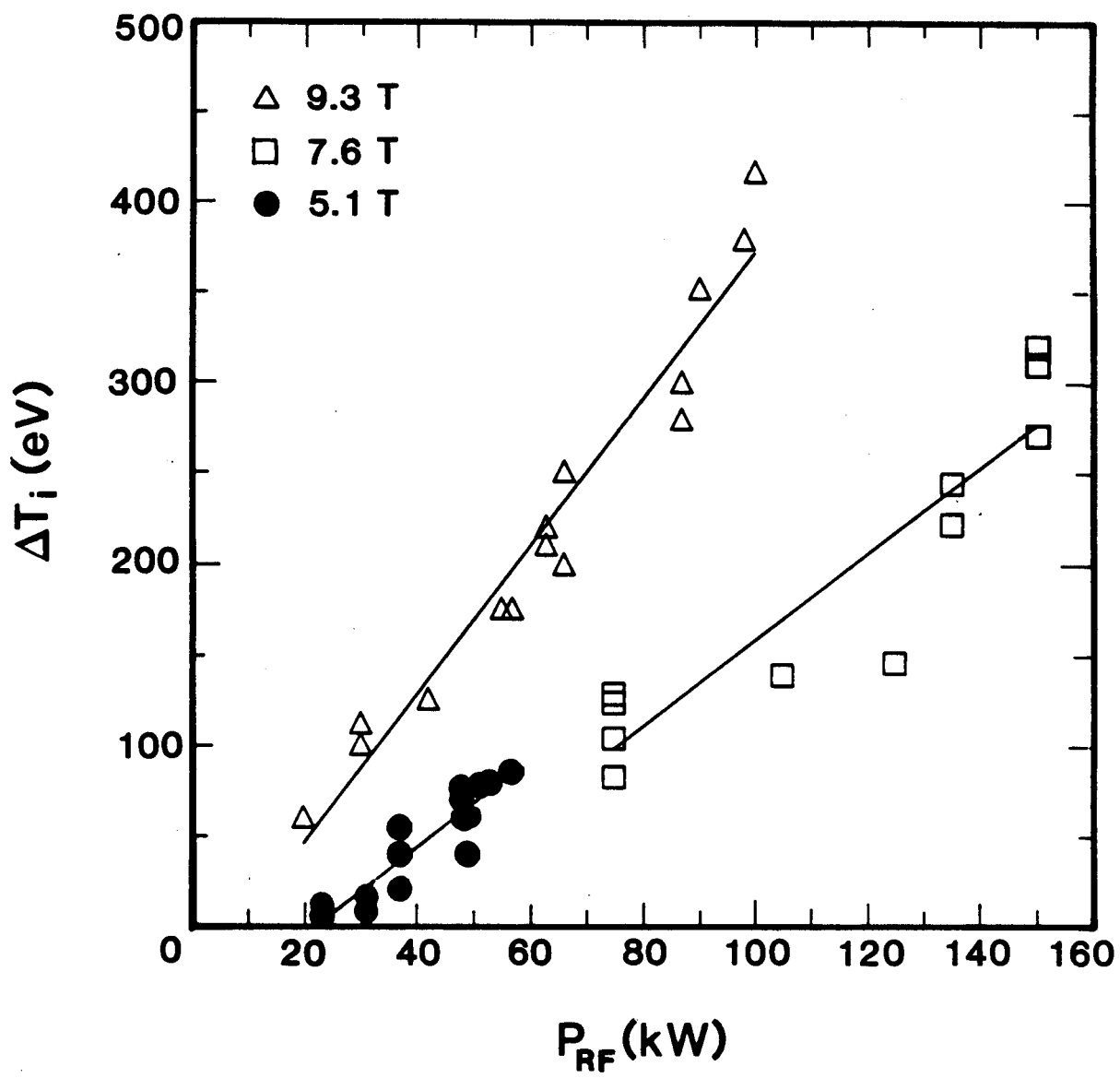


Fig. 1



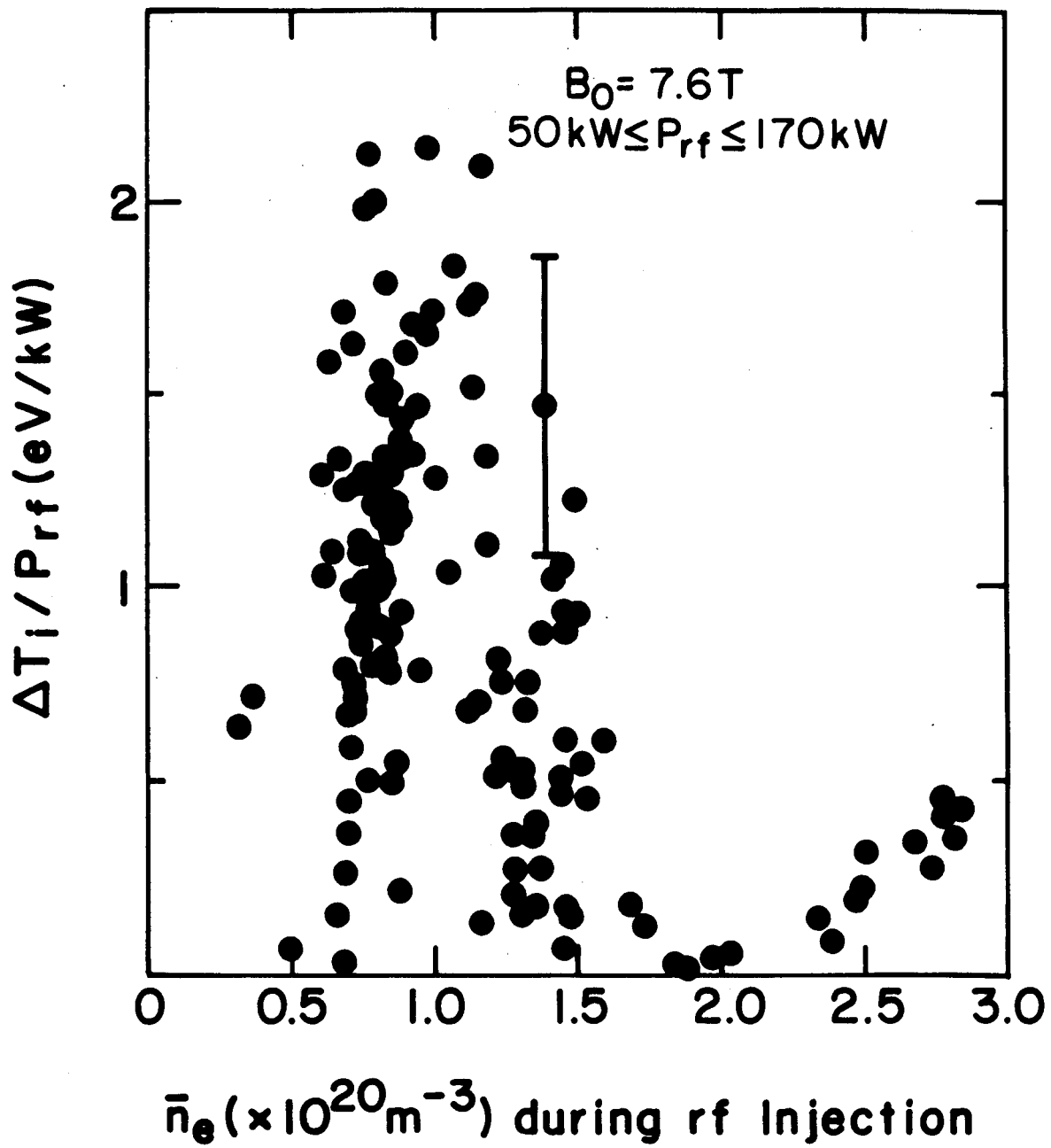


Fig. 2(b)

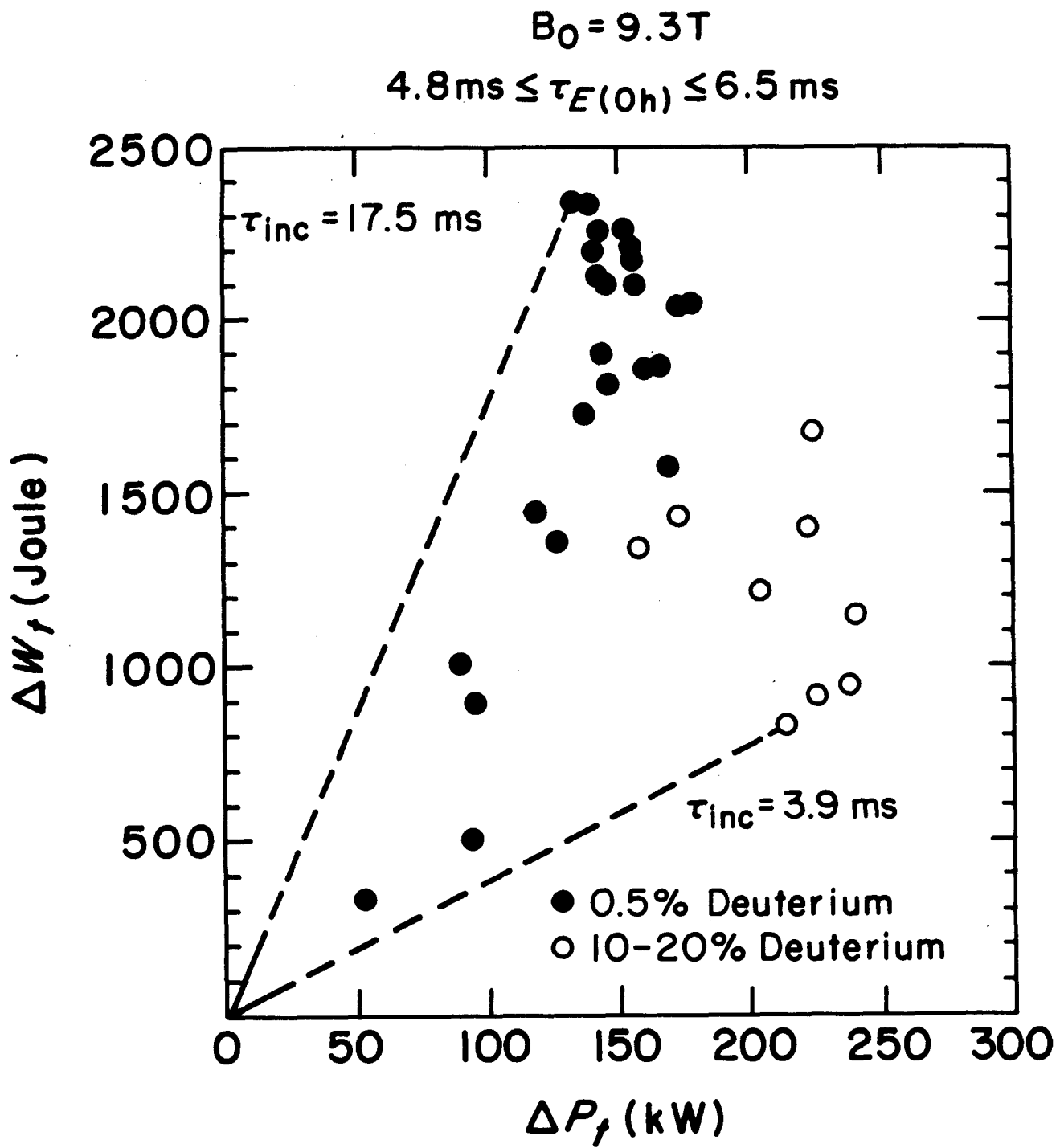


Fig. 3